Metal Binding Within a Peptide-Based Nucleobase Stack with Tuneable Double-Strand Topology

Andrea Küsel,[a] Jinhua Zhang,[a] Miguel Alvariño Gil,[b] A. Claudia Stückl,[b] Wolfram Meyer-Klaucke,[c] Franc Meyer,*[b] and Ulf Diederichsen*[a]

Keywords: EXAFS spectroscopy / Molecular recognition / Nucleic acids / Peptides / Protein models

Peptide nucleic acid (PNA) oligomers with linear topology are synthesised with histidines at the central positions in order to provide metal-ion coordination sites within the water shielded and non-polar environment of a nucleobase stack that emerges upon duplex formation. Variation of the linker length used for attachment of the nucleobases to the regular peptide backbone allows for fine tuning of the distances and coordination environment at the metal binding site. The effect of zinc and copper incorporation into the modified alanyl-PNA scaffolds on duplex stability was probed by temperature-dependent UV spectroscopy, and additional insight was gained from EPR spectroscopy and EXAFS. Whenever four histidines (two per oligomer strand) are available, addition of Zn^{2+} significantly enhances double-strand stability, thus supporting coordination of Zn^{2+} by the histidine-N and incorporation of the metal ion within the base stack. In contrast to Zn^{2+}, however, Cu^{2+} ions do not induce double-strand formation of an alanyl/norvalyl-PNA oligomer, as confirmed by EPR and EXAFS, which reveal a mixed $\{N_2O_x\}$ donor environment. While metal-ion binding to histidine-modified alanyl-PNA oligomers (and homologues) is apparently feasible, a proper matching of the binding-site geometry and the stereoelectronic requirements of the specific metal ion are essential in order to mediate double-strand formation. This might offer new options for alternative pairing schemes in alanyl-PNA chemistry in which metal coordination substitutes the common base-pair H-bonding pattern, and for metal-dependent regulation of alanyl-PNA duplex formation.

Introduction

Artificial DNA, in which one or multiple nucleosides is replaced by so-called "ligandosides" capable of metal-ion binding, is receiving increasing attention.[1–3] Inter alia, metal-mediated base pairing is exploited in order to increase the thermal stability of the DNA duplex, to extend the genetic alphabet for DNA-based information storage, or to develop novel nanostructured metal-containing architectures with interesting physical properties.[4] Peptide nucleic acids (PNAs) are synthetic analogues of nucleic acids with a non-natural polyamide backbone, most commonly based on *N*-(2-aminoethyl)glycine.[5] Their particularly attractive properties comprise self-recognition, high chemical and biological stability, and strong binding to target DNA or RNA sequences. Recently, some high affinity metal-binding sites such as porphyrins,[6] bipyridines[7,8] or chelating amines[9–11] and organometallic moieties[12] have been appended to PNA, and these metal complex/PNA conjugates have been probed in the context of sequence-specific DNA/RNA cleavage and detection,[6,8,13] DNA-templated catalysis,[10] and for the development of new antisense drugs.[14] In most of these systems the ligand site for metal binding is attached to one end of the PNA strand, but it has also been shown that metal incorporation in the middle of complementary *N*-(2-aminoethyl)glycine PNA strands that have been modified by bipyridine is indeed feasible and leads to preservation of the helical duplex structure.[7]

In the present contribution we probe hitherto unexplored metal incorporation into alanyl peptide nucleic acids (alanyl-PNA). Alanyl-PNA is structurally based on a regular peptide composed of alanyl amino acids with alternating configuration and nucleobases covalently linked to methylene side-chains.[15–17] Double strands are formed by two complementary alanyl-PNA strands based on base-pair recognition, stacking and solvation. The duplexes need to adopt a linear double-strand topology since the distance between consecutive side-chains in an extended peptide is close to the ideal base-pair stacking distance. The resulting alanyl-PNA double strand with linear topology is well defined regarding nucleobase orientation and distances and it is limited with respect to conformational freedom. Further-

[a] Institut für Organische und Biomolekulare Chemie, Georg-August-Universität Göttingen,
Tammannstraße 2, 37077 Göttingen, Germany
Fax: +49-551-392-944
E-mail: udieder@gwdg.de
[b] Institut für Anorganische Chemie, Georg-August-Universität Göttingen,
Tammannstraße 4, 37077 Göttingen, Germany
Fax: +49-551-393-063
E-mail: franc.meyer@chemie.uni-goettingen.de
[c] European Molecular Biology Laboratory, Outstation Hamburg, Notkestraße 85, 22603 Hamburg, Germany

more, chromophores incorporated within the nucleobase stack are known to be significantly shielded from aqueous solution.[18]

Coordination of metal ions within the nucleobase stack is especially interesting, since the non-polar environment inside the base stack should have unique consequences for the stability and geometry of metal coordination. The alanyl-PNA framework offers the particular advantage of being able to use natural amino acids such as histidine as biomimetic metal binding sites at different positions of the strand. Metal ions in such a metalloenzyme-inspired water-shielded environment might be useful for, inter alia, catalytic applications, while the alanyl-PNA backbone and nucleobases offer additional possibilities for specific substrate recognition via hydrogen-bonding interactions. This investigation might also be of interest to establish specific metal-mediated recognition next to hydrogen bonding in double-strand interactions. Finally, homologation of the side-chains in alanyl-PNA might allow for fine tuning of the distances and geometries of the metal binding sites or even the possibility to introduce dinuclear metal arrays.

Here, various alanyl-PNAs and side-chain homologous oligomers with central histidine metal binding sites are presented and investigated with respect to their ability to stabilize double-strand formation mediated by metal ions. It should be noted that in the absence of high-affinity ligands the amide groups in the PNA backbone and the nucleobases may act as competing binding sites for metal ion complexation,[19] and various spectroscopic and analytical tools are thus required in order to clearly characterise metal incorporation into the modified PNA duplexes.

Results and Discussion

Double-strand formation of an alanyl-PNA hexamer based on Watson–Crick pairing of six G-C base pairs is

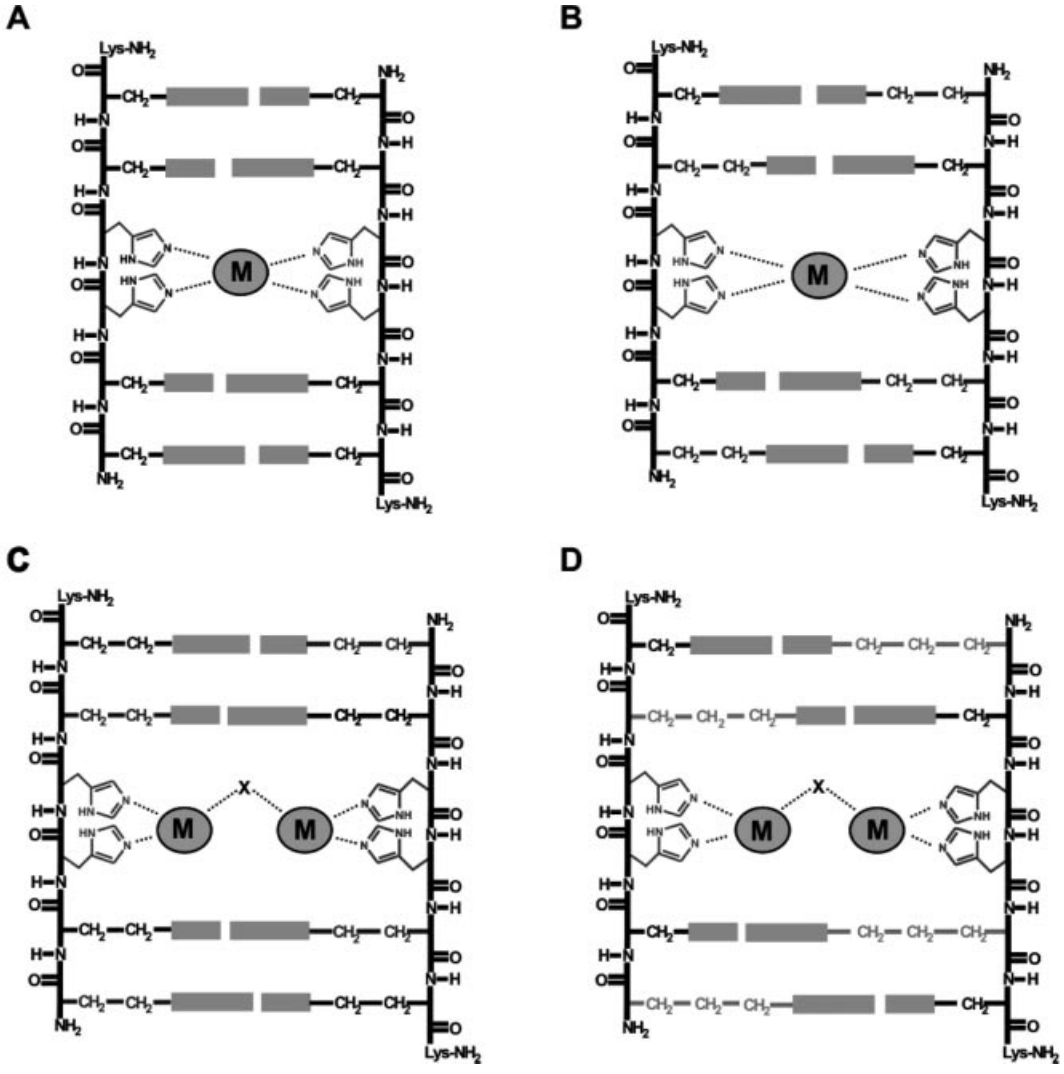

Figure 1. Idealized representation of double strands with a linear topology based on a peptide backbone with alternating amino acid configuration, four G-C base pairs and central histidines as metal ion coordination sites. Alanyl-peptide nucleic acids (alanyl-PNAs) should allow for coordination of one metal ion (**A**) as should alanyl/homoalanyl mixed PNAs (**B**). The distance of histidine coordination sites in homoalanyl-PNA might allow incorporation of two metal ions (**C**); the metal binding geometry in mixed alanyl/norvalyl-PNAs should be comparable (**D**). X might be a small bridging ligand such as HO^-, Cl^- or AcO^-.

known to be quite stable (T_m = 58 °C).[16] Therefore, it was likely that an exchange of the central two G-C base pairs for histidine side-chains would retain the ability for duplex formation. In alanyl-PNA and mixed alanyl/homoalanyl-PNA double strands with four central histidines, coordination of one metal ion can be expected based on a backbone distance of about 14–15 Å (Figure , A and B). The backbone distance is extended to about 16.5 Å by further side-chain homologation, possibly allowing for two metal coordination sites. Therefore, homoalanyl-PNA and alanyl/norvalyl-PNA with central histidines were prepared (Figure 1, C and D).

Alanyl-PNA oligomers **1**–**3** as well as the side-chain homologous alanyl/homoalanyl-PNAs **4**–**6**, homoalanyl-PNAs **7** and **8** and alanyl/norvalyl-PNA oligomers **9** and **10** (Table 1) were prepared by manual solid-phase peptide synthesis based on a Boc strategy.[20] The respective nucleobase-substituted amino acids were assembled on an MBHA polystyrene support using HATU as the coupling reagent. The oligomers were purified by HPLC and characterised by mass spectrometry.

Double-strand formation was investigated by temperature-dependent UV spectroscopy. This method relies on a sigmoidal increase of UV absorption with higher temperatures caused by a cooperative destacking of the nucleobases. It was adapted from oligonucleotide chemistry and has been used successfully for the characterisation of PNA double strands.

Alanyl-PNA Oligomers

In the alanyl-PNA series enantiomeric oligomers provide tridentate G-C Watson–Crick pairing, as has been shown for an equimolar mixture of hexamers **1** and ***ent*-1** (T_m = 58 °C).[16] In contrast, nucleo amino acids with a different configuration form the less stable G-C reverse Watson–Crick base pair (self pairing of **1**: T_m = 42 °C).[16] Therefore, the enantiomeric oligomers **2** and ***ent*-2** were prepared, both of which feature two histidines in central positions. Watson–Crick self-pairing as well as equimolar pairing of enantiomers **2** and ***ent*-2** turned out not to be stable enough for detection of double-strand formation. Nevertheless, in the presence of Zn^{2+} ions UV melting curves clearly indicate self-pairing of **2** and pairing of enantiomeric oligomers **2** and ***ent*-2**, both with a stability of about 15 °C (Figure 2, A). Zinc ions obviously interact with the respective oligomers in order to overcome the low double-strand stability.

Table 1. Synthesized peptide nucleic acid oligomers with their double-strand stabilities in the absence or presence of Zn^{2+} ions.

Oligomers[a]	No.	T_m	T_m with Zn^{2+}
H-(AlaG-AlaG-AlaC-AlaG-AlaC-AlaC)-Lys Lys-(AlaC-AlaC-AlaG-AlaC-AlaG-AlaG)-H	**1** ***ent*-1**	58 °C[b]	
H-(AlaG-AlaC-**His**-**His**-AlaG-AlaC)-Lys Lys-(AlaC-AlaG-**His**-**His**-AlaC-AlaG)-H	**2**	< 0 °C[b]	15 °C[b]
H-(AlaG-AlaC-**His**-**His**-AlaG-AlaC)-Lys Lys-(AlaC-AlaG-**His**-**His**-AlaC-AlaG)-H	**2** ***ent*-2**	< 0 °C[b]	15 °C[b]
H-(AlaG-AlaC-**His**-**Gly**-AlaG-AlaC)-Lys Lys-(AlaC-AlaG-**Gly**-**His**-AlaC-AlaG)-H	**3**	13 °C[b]	13 °C[b]
H-(AlaG-AlaC-**His**-**His**-AlaG-AlaC)-Lys Lys-(AlaC-AlaG-**Gly**-**His**-AlaC-AlaG)-H	**2** **3**	15 °C[b]	14 °C[b]
H-(AlaC-HalC-AlaG-HalC-AlaG-HalG)-Lys Lys-(HalG-AlaG-HalC-AlaG-HalC-AlaC)-H	**4**	52 °C[b]	
H-(HalG-AlaC-**His**-**His**-HalG-AlaC)-Lys Lys-(AlaC-HalG-**His**-**His**-AlaC-HalG)-H	**5**	< 0 °C[b] < 0 °C[c]	17 °C[b] 12 °C[c]
H-(AlaC-HalC-AlaG-**His**-**His**-HalC-AlaG-HalG)-Lys Lys-(HalG-AlaG-HalC-**His**-**His**-AlaG-HalC-AlaC)-H	**6**	12 °C[c]	24 °C[c]
H-(HalG-HalG-HalC-HalG-HalC-HalC)-Lys Lys-(HalC-HalC-HalG-HalC-HalG-HalG)-H	**7** ***ent*-7**	32 °C[b]	
H-(HalG-HalC-**His**-**His**-HalG-HalC)-Lys Lys-(HalC-HalG-**His**-**His**-HalC-HalG)-H	**8**	< 0 °C[b] < 0 °C[c]	15 °C[b] 8 °C[c]
H-(AlaG-NvaG-AlaC-NvaG-AlaC-NvaC)-Lys Lys-(NvaC-AlaG-NvaG-AlaC-NvaG-AlaG)-H	**9** ***ent*-9**	16 °C[b]	
H-(AlaC-NvaC-AlaG-**His**-**His**-NvaC-AlaG-NvaG)-Lys Lys-(NvaG-AlaG-NvaC-**His**-**His**-AlaG-NvaC-AlaC)-H	**10**	11 °C[b] 17 °C[c]	22 °C[c]
H-(AlaC-NvaC-AlaG-**His**-**His**-NvaC-AlaG-NvaG)-Lys Lys-(NvaG-AlaG-NvaC-**His**-**His**-AlaG-NvaC-AlaC)-H	**10** ***ent*-10**	15 °C[b] 21 °C[c]	27 °C[c]

[a] AlaG = β-(9-guaninyl)alanine, AlaC = β-(1-cytosinyl)alanine, HalG = γ-(9-guaninyl)homoalanine, HalC = γ-(1-cytosinyl)homoalanine, NvaG = δ-(9-guaninyl)norvaline, NvaC = δ-(1-cytosinyl)norvaline; nucleobase-substituted amino acids with a D-configuration are underlined. [b] Phosphate buffer (0.01 M Na_2HPO_4/H_3PO_4, 0.1 M NaCl, pH 7). [c] HEPES buffer (0.01 M HEPES, 0.1 M NaCl, pH 7).

In the absence of zinc, however, the non-coordinating histidines seem to suppress double-strand formation, presumably because of charge repulsion of the protonated side-chains at physiological pH; one should note that double-strand formation with considerable stability is known for G-C alanyl-PNA tetramers.[16]

Oligomer **3**, which features a histidine next to a glycine in the central position, was synthesised with the intention to test oligomers with lower potential for zinc coordination. Interestingly, self-pairing was now provided with a stability of T_m = 13 °C and it was not possible to increase this stability by zinc addition. First of all, this is an argument for the charge repulsion of neighbouring histidines hampering formation of double strands in the case of oligomer **2**. Furthermore, the lack of double-strand stabilisation upon addition of zinc to oligomer **3** is in agreement with two histidines not being sufficient for incorporation of zinc. Coordination at the nucleobases can be excluded as a reason for the stabilisation of double strands formed by oligomers **2** and ***ent*-2**, which only occurs in the presence of zinc ions. This result was confirmed by homochiral Watson–Crick pairing of oligomers **2** and **3** providing a potential zinc binding centre of three histidines: in agreement with the more stable pairing mode and possible charge repulsion of neighbouring histidines, the double strand **2** + **3** without zinc ions was formed only with slightly higher stability (T_m = 15 °C) than self-pairing of oligomer **3**, whereas addition of zinc had no effect on the overall stability (T_m = 14 °C).

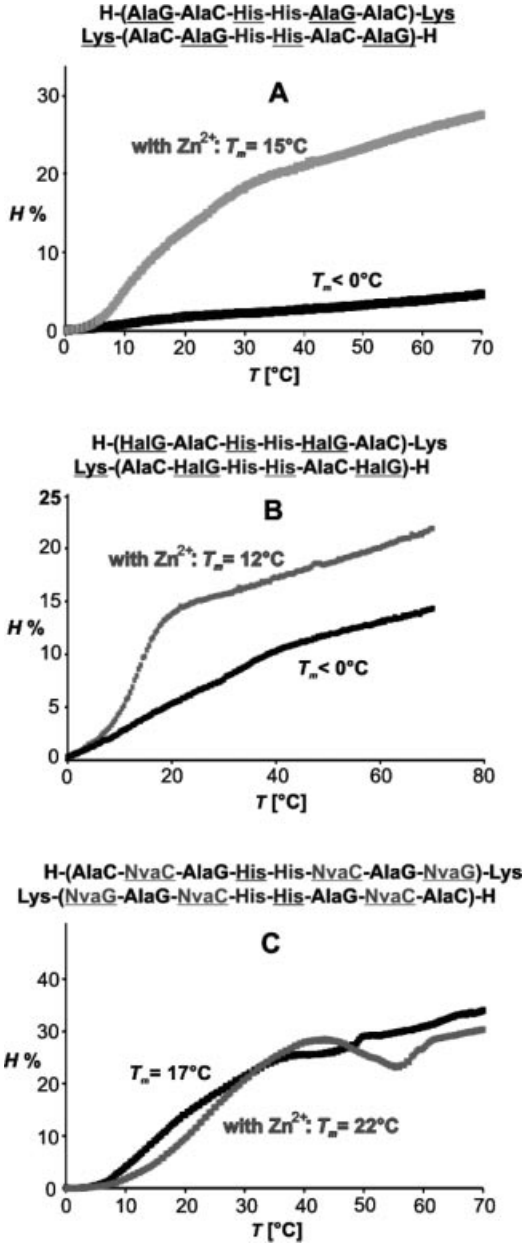

Figure 2. UV melting curves of alanyl-PNA (**2**) in phosphate buffer (A) and of alanyl/homoalanyl-PNA (**5**; B) as well as alanyl/norvalyl-PNA (**10**; C) in HEPES buffer in the absence (dark curves) or presence (light curves) of Zn^{2+}.

Mixed Alanyl/Homoalanyl-PNA Oligomers

Peptide nucleic acid double strands composed of alternating alanyl and homoalanyl nucleo amino acids provide a backbone distance that is about 1 Å larger than alanyl-PNA duplexes. This should significantly influence metal coordination by the central histidines. Furthermore, in the mixed alanyl/homoalanyl-PNA series the more stable Watson–Crick G-C base pairs are formed with self-pairing homodimers.[20] A stability of T_m = 52 °C was found for the homodimer of hexamer **4**. Like in alanyl-PNA, the exchange of the central G-C base pairs for four histidines in the double strand of oligomer **5** prevents double-strand formation. Addition of zinc ions to oligomer **5** leads to stabilisation (T_m = 17 °C) of the same order of magnitude as observed for the respective alanyl-PNA **2**.

Since a possible application of the metal/PNA conjugates will be the catalysis of, inter alia, phosphodiester hydrolysis, the double-strand stabilities were also investigated in HEPES buffer instead of the more common phosphate buffer in order to evaluate the effect of the medium. In HEPES buffer double-strand formation of oligomer **5** was again not observed and zinc ions turned out to be essential for stabilisation (T_m = 12 °C; Figure 2, B). However, the change from phosphate to HEPES buffer resulted in a 5 °C decrease of stability.

With the aim of providing double strands with a higher overall stability, the mixed alanyl/homoalanyl-PNA oligomer **6**, which features six nucleo amino acids and two central histidines, was prepared. The low double-strand stability of the homodimer **6** (T_m = 13 °C) resembles the effect of four non-coordinating histidines in the central region, as mentioned already in the alanyl-PNA series. Addition of zinc ions leads to a significant increase in stability (T_m = 25 °C) even in HEPES buffer, which makes this system a promising candidate for further studies.

Homoalanyl-PNA and Mixed Alanyl/Norvalyl-PNA Oligomers

Both homoalanyl-PNA as well as mixed alanyl/norvalyl-PNA double strands provide a distance between the peptide

backbones that is determined by the base-pair size extended by overall four methylene units (Figure 1, C and D). This might open the possibility for coordination of two zinc ions within the centre of a linear PNA double strand. In the homoalanyl-PNA series, double-strand formation with nucleobases having the same configuration (homochiral base pairing) leads to the more stable G-C Watson–Crick pairing.[20] The double strand of homoalanyl-PNA enantiomers **7** and ***ent*-7** with six G-C base pairs provides a stability of T_m = 32 °C. The drop of stability compared to the alanyl and alanyl/homoalanyl-PNAs **1** and **4** is caused by higher side-chain flexibility and lower stacking contributions.[20] As a consequence, double-strand formation of homoalanyl-PNA **8** was not observed since it would only be based on four poorly stacked reverse Watson–Crick G-C base pairs with four histidine amino acids in the centre. Considering the poor situation for self-pairing, it is even more remarkable that addition of zinc ions to oligomer **8** induced duplex formation with a similar order of stability as observed for alanyl/homoalanyl oligomer **5** (T_m = 15 °C in phosphate and T_m = 8 °C in HEPES buffer).

The stabilities of the G-C Watson–Crick pairing homoalanyl-PNA hexamer double strand **7** + ***ent*-7** (T_m = 32 °C) and the respective alanyl/norvalyl-PNA duplex **9** + ***ent*-9** (T_m = 16 °C) are quite different despite a similar overall double-strand geometry.[20] The lower degree of side-chain preorganisation in the case of the norvalyl amino acids seems to be responsible for this effect. In analogy to oligomer **6**, the alanyl/norvalyl-PNA oligomers **10** and ***ent*-10**, with six nucleo amino acids and two central histidines, were prepared for the investigation of zinc binding. Reverse Watson–Crick pairing was provided with a stability of T_m = 17 °C in the absence of zinc, whereas the stability of the mixture of enantiomers **10** and ***ent*-10** forming the more stable Watson–Crick base pairs was even higher at T_m = 22 °C. The larger backbone distance in alanyl/norvalyl-PNA provides reduced charge interaction for opposed central histidines. In contrast to oligomers **2** and **5**, this allows for stable duplex formation without zinc binding. For both alanyl/norvalyl-PNA oligomers **10** and **10** + ***ent*-10** the addition of zinc leads to a significant increase in double-strand stability of 5 or 6 °C, respectively.

In order to provide additional information on the metal ion binding potential of oligomer **10**, this particular system was studied in more detail by spectroscopic methods in solution. Since Zn^{2+} is spectroscopically silent, Cu^{2+} was used instead. It should be noted, though, that according to the temperature-dependent UV spectra, double-strand formation was not induced by the addition of copper salts to oligomer **10** (data not shown).

EPR spectroscopy was used as a qualitative probe to verify the binding of Cu^{2+} by PNA **10**. Part a of Figure 3 shows the X-band EPR spectra of a solution of Cu^{2+} only (top) and of a solution of oligomer **10** with 1 equiv. of Cu^{2+} (bottom) in HEPES-buffered water/glycerine (3:1). A much smaller value for $A_z(^{63,65}Cu)$ in the presence of oligomer **10** is clearly discernible, thus confirming coordination of Cu^{2+}. Both the g_z and A_z values are within the range expected

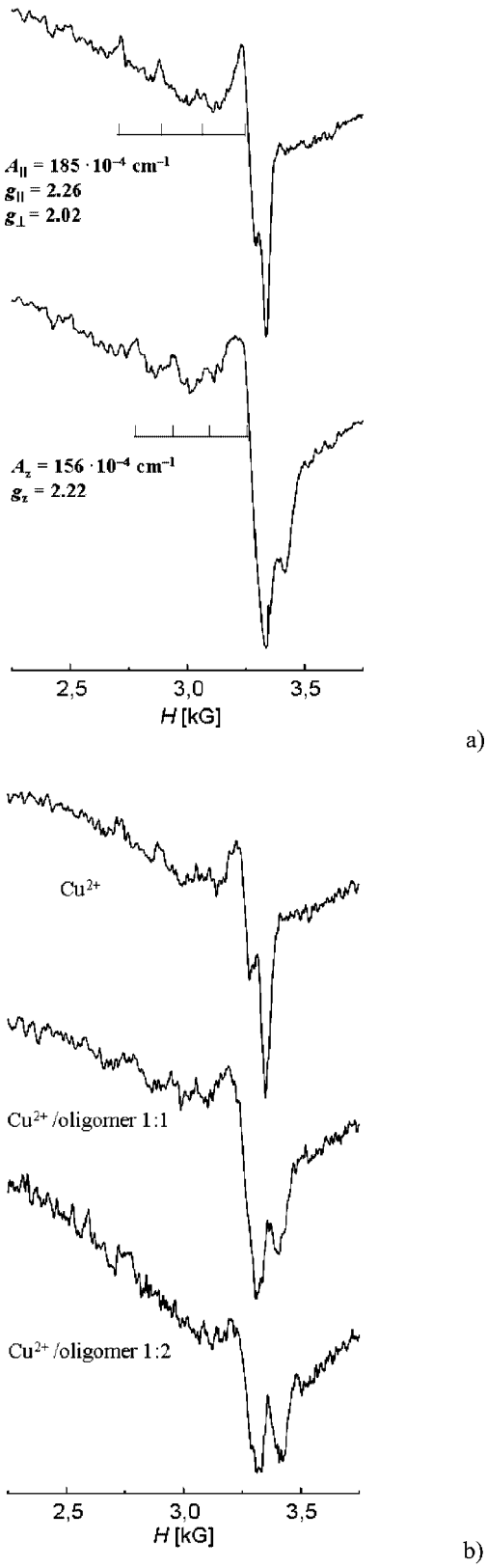

Figure 3. a) EPR spectra of Cu^{2+} in the absence or presence of **10**: H_2O/glycerin (3:1), HEPES pH 7, 150 K; only Cu^{2+} (top) or Cu^{2+}/**10** (1:1, bottom). b) EPR spectra of Cu^{2+} in the absence or presence of **10**: H_2O, HEPES pH 7.4, 150 K; only Cu^{2+} (top), Cu^{2+}/**10** (1:1, middle) or Cu^{2+}/**10** (1:2, bottom).

for some mixed $\{N_xO_y\}$ ligation,[21] but no ^{14}N hyperfine coupling could be detected and no satisfactory simulation of the data could be achieved because of, inter alia, a relatively low signal-to-noise ratio.[22] In addition, the spectra in water at different ratios of Cu^{2+} to PNA **10** (Figure 3, b) indicated the possible presence of several species, leaving the EPR confirmation of metal ion binding by oligomer **10** only a qualitative one.

Cu^{2+} coordination by the histidine N-atoms of PNA **10** was further substantiated by X-ray absorption spectroscopy conducted on a frozen sample of oligomer **10**/Cu^{2+}. X-ray absorption spectroscopy allows the element-specific characterisation of metal environments and thus yields information about the type and distances of coordinating ligands. Ligands with a rather linear arrangement of the backscattering atoms lead to special features in the spectrum due to multiple scattering of the photoelectron wave that is created upon absorption of photons with energies larger than the edge energy. Here, a flat plateau at $k \approx 4.5$ Å^{-1} indicates the presence of imidazole groups coordinating the metal ion. This was further supported by the Fourier transform of the spectrum. The intense contribution at about 4 Å arises from scattering events at the remote atoms of the imidazole rings. Their intensity was increased due to the multiple scattering events including the metal coordinating nitrogen atom. The first coordination shell has a typical distance of about 2.0 Å and its high intensity indicates a homogeneous coordination by light atoms (C/N or O).

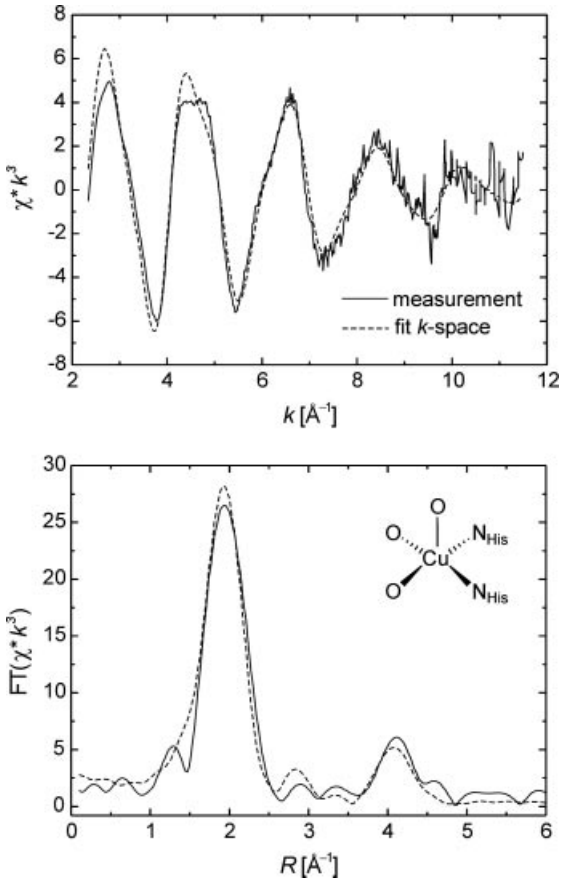

Figure 4. EXAFS and corresponding Fourier transform for the PNA **10**/Cu^{2+} complex (black). The best fit to the data is shown in dashed lines and represents coordination by two imidazole groups and three oxygen atoms.

With this in mind, different combinations of O and imidazole ligands were modelled to the data. The final model given in Figure 4 comprises two imidazole groups and three oxygen ligands at a distance of 1.98 Å. In order to keep the number of free parameters as low as possible the distances for these ligands as well as their Debye–Waller factors ($2\sigma^2 = 0.021$ Å^2) were constrained. Thus, the measurement is not resembled in all details, but any over-interpretation of data is prevented. Typical errors for the coordination number are in the range of 20%, whereas the distances have an error of less than 1% for the first coordination sphere.

Conclusions

A series of alanyl-, homoalanyl- and norvalyl-PNA hexamers or octamers has been prepared in which two central nucleobase-substituted amino acids are replaced by histidines. While the incorporation of histidine residues is shown to drastically lower the tendency for self-pairing compared to the parent PNAs, double-strand formation is still observed for properly chosen systems that provide at least six G-C pairs framing the central histidines (such as in **6**, **10** or **10**/***ent*-10**). As soon as four histidines (two per oligomer strand) are placed at the centre of PNA double strands, addition of Zn^{2+} significantly enhances the duplex stability, thus supporting the coordination of Zn^{2+} by the histidine-N and incorporation of the metal ion within the base stack (Figure 5). Metal ion binding to the histidine-N of the modified alanyl/norvalyl-PNA oligomers is further supported by ESR and EXAFS spectroscopy on the corresponding Cu^{2+} hybrid of **10**. In contrast to Zn^{2+}, however, Cu^{2+} ions do not induce double-strand formation, in accordance with the mixed $\{N_2O_x\}$ donor environment that was deduced from EPR and EXAFS experiments (Figure 5). One might speculate that the different geometric preferences of Zn^{2+} and Cu^{2+} upon binding to four histidine-N (tetrahedral for Zn^{2+}, square planar for Cu^{2+}) give rise to these different effects. It should be noted that for modified DNA it has also been observed that duplex formation is mediated by only specific metal ions.[3]

The present findings thus confirm the anticipated metal ion binding capabilities of histidine-modified alanyl-PNA oligomers (and homologues), i.e. metal binding to conjugates of alanyl-PNA and natural amino acids. However, proper organisation of the metal binding site is essential in order to match the stereoelectronic requirements of the specific metal ion upon double-strand formation. This might offer new options for alternative pairing schemes in alanyl-PNA chemistry in which metal coordination substitutes the common base-pair H-bonding pattern, and for metal-dependent regulation of alanyl-PNA duplex formation.

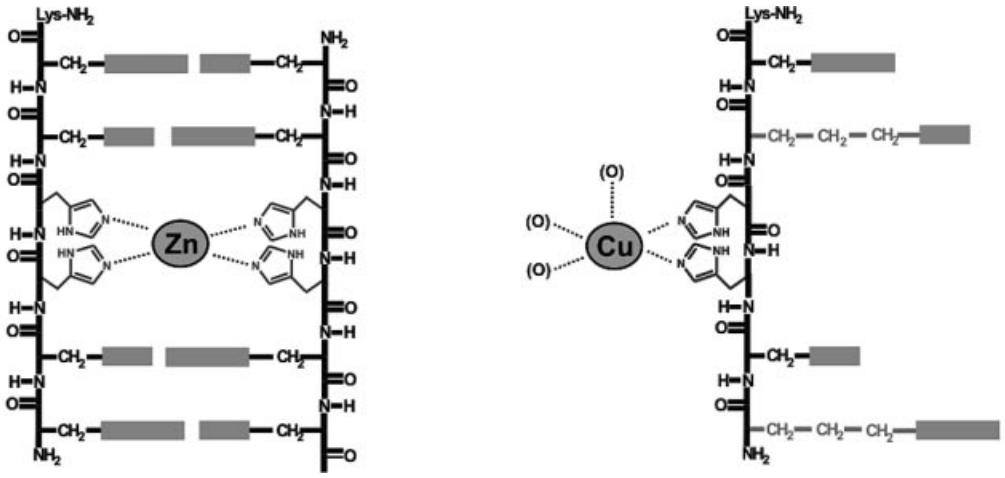

Figure 5. Likely binding modes of Zn^{2+} and Cu^{2+} to histidine-modified alanyl-PNA.

Experimental Section

General Remarks: All reagents were of analytical grade and used as supplied. Solvents were of the highest grade available. Synthesis and analytical data of *N*-Boc-AlaG-OH, *N*-Boc-AlaC(*Z*)-OH, *N*-Boc-HalG-OH, *N*-Boc-HalC(*Z*)-OH, *N*-Boc-NvaG-OH and *N*-Boc-NvaC(*Z*)-OH were performed as described previously.[20] (*S*)-*N*-Boc-His(Bom)-OH and (*R*)-*N*-Boc-His(Bom)-OH were purchased from Bachem.

ESI mass spectra were recorded with a TSQ 700 Finnigan spectrometer and high resolution mass spectra with a Bruker Apex IV FT-ICR MS instrument. HPLC was done on a Pharmacia Äkta Basic using YMC-Pack ODS, RP-C18 with a linear gradient of A (0.1% TFA in water) to B (0.1% TFA in acetonitrile/water, 9:1). Oligomers were purified using 250 × 20 mm, 5 μm, 120 Å for preparative and 250 × 4.6 mm, 5 μm, 120 Å columns for analytical samples. UV melting curves were measured with a Perkin–Elmer UV/Vis Lambda 10 with a Peltier temperature programmer PTP 1 or a Jasco V-550 UV/Vis spectrometer equipped with a Jasco ETC-505S/ETC-505T temperature controller. The oligomer concentration was determined by taking the extinction coefficient at 80 °C as being the sum of the extinction coefficients of all nucleo amino acids.[20] Complex formation was achieved by heating to 85 °C, followed by slow cooling over a period of three hours to 0 °C and equilibration for at least three hours at 0 °C. EPR spectra were measured on a Bruker ELEXSYS E500 spectrometer, equipped with a digital temperature control system ER 4131 VT using nitrogen as coolant. All spectra at 150 K were recorded at about 9.4 GHz microwave frequency, 5–9 G field modulation amplitude, 100 kHz field modulation frequency, and around 10 mW microwave power. Glycerine was added to some of the samples to improve their freezing behaviour. To induce complex formation, the same procedure was used as in the case of UV/Vis spectroscopy immediately before recording the spectra.

General Method for Solid-Phase Peptide Synthesis (SPPS) of the Oligomers: Oligomerisation was performed as a solid-phase peptide synthesis on a 4-methylbenzhydrylamine (MBHA)-polystyrene resin loaded with (*S*)-*N*-*tert*-butoxycarbonyl-lysine(2-Cl-Z)-OH (0.43 mmol/g) or (*R*)-*N*-Boc-lysine(*Z*)-OH (0.57 mmol/g) in a small column. For each step, 5 equiv. of *N*-Boc-protected amino acid was used and activated by 4.5 equiv. of *N*-(7-azabenzotriazol-1-yl)-1,1,3,3-tetramethyluronium hexafluorophosphate (HATU) and 5 equiv. of 1-hydroxy-7-azabenzotriazol (HOAt) in DMF (600–1000 μL). After 3 min, 10 equiv. of *N*,*N*-diisopropylethylamine was added.

After swelling the resin for 1 h in CH_2Cl_2, the following strategy was repeated for every amino acid unit: 1) Deprotection: The resin was washed with TFA/*m*-cresol (95:5, 2 mL) and then treated with TFA/*m*-cresol (95:5, 2 mL) for 5 min. 2) Washing: CH_2Cl_2/DMF (1:1; 5 × 2 mL) followed by pyridine (2 × 2 mL). 3) Coupling: The reaction column was gently moved for 30–90 min with the coupling reagents (30 min for natural amino acids, 45 min for cytosine-containing amino acids, 90 min double coupling for guanine-containing amino acids). 4) Washing: CH_2Cl_2/DMF (1:1; 5 × 2 mL), DMF/piperidine (9:1; 5 × 2 mL), CH_2Cl_2/DMF (1:1; 5 × 2 mL). 5) Capping: 2 × 5 min with Ac_2O/NEt_3/DMF (1:1:8; 2 mL). 6) Washing: CH_2Cl_2/DMF (1:1; 5 × 2 mL), DMF/piperidine (9:1; 5 × 2 mL), CH_2Cl_2/DMF (1:1, 5 × 2 mL). Finally, the resin was washed with MeOH and dried for 3 h over KOH. Cleavage from the solid support was carried out within 2 h using trifluoromethanesulfonic acid/*m*-cresol/TFA (1:1:8; 2 mL). The dark brown solution was concentrated to 300 μL and the peptide nucleic acids were precipitated with diethyl ether (10–20 mL) as a white solid. The PNA was separated using a centrifuge, followed by purification with HPLC (RP-C18).

H-(AlaG-AlaC-His-His-AlaG-AlaC)-Lys-NH_2 (2): HPLC (gradient: 5–30% B in 30 min): t_R = 11.54 min. ESI-MS: *m*/*z* = 1220.7 $[M + H]^+$, 611.2 $[M + 2H]^{2+}$. HRMS: calcd. for $C_{48}H_{61}N_{29}O_{11}$ $[M + 2H]^{2+}$ 610.76254; found 610.76220.

H-(AlaG-AlaC-His-His-AlaG-AlaC)-Lys-NH_2 (*ent*-2): HPLC (gradient: 5–30% B in 30 min): t_R = 11.67 min. ESI-MS: *m*/*z* = 1220.8 $[M + H]^+$, 611.2 $[M + 2H]^{2+}$. HRMS: calcd. for $C_{48}H_{61}N_{29}O_{11}$ $[M + 3H]^{3+}$ 407.51079; found 407.51079.

H-(AlaG-AlaC-His-Gly-AlaG-AlaC)-Lys-NH_2 (3): HPLC (gradient: 5–30% B in 30 min): t_R = 10.19 min. ESI-MS: *m*/*z* = 1140.6 $[M + H]^+$, 571.4 $[M + 2H]^{2+}$. HRMS: calcd. for $C_{44}H_{57}N_{27}O_{11}$ $[M + 2H]^{2+}$ 570.74382; found 570.74371.

H-(HalG-AlaC-His-His-HalG-AlaC)-Lys-NH_2 (5): HPLC (gradient: 5–30% B in 30 min): t_R = 12.50 min. ESI-MS: *m*/*z* = 1276.9 $[M + H]^+$, 639.2 $[M + 2H]^{2+}$. HRMS: calcd. for $C_{52}H_{69}N_{29}O_{11}$ $[M + 2H]^{2+}$ 638.79384; found 638.79362.

H-(AlaC-HalC-AlaG-His-His-HalC-AlaG-HalG)-Lys-NH_2 (6): HPLC (gradient: 5–25% B in 20 min): t_R = 14.19 min. ESI-MS:

m/z = 1662.8 $[M + H]^+$, 832.2 $[M + H]^{2+}$. HRMS: calcd. for $C_{66}H_{83}N_{39}O_{15}$ $[M + 3H]^{3+}$ 554.90497; found 554.90492.

H-(HalG-HalC-His-His-HalG-HalC)-Lys-NH_2.(8): HPLC (gradient: 5–30% B in 30 min): t_R = 12.50 min. ESI-MS: *m/z* =1276.6 $[M + H]^+$, 639.5 $[M + 2H]^{2+}$.

H-(AlaC-NvaC-AlaG-His-His-NvaC-AlaG-NvaG)-Lys-NH_2 (10): HPLC (gradient: 5–25% B in 20 min): t_R = 13.55 min. ESI-MS: *m/z* =853.2 $[M + H]^{2+}$, 569.3 $[M + 2H]^{3+}$. HRMS: calcd. for $C_{69}H_{89}N_{39}O_{15}$ $[M + 3H]^{3+}$ 568.92062; found 568.92063.

H-(AlaC-NvaC-AlaG-His-His-NvaC-AlaG-NvaG)-Lys-NH_2 (*ent*-10): HPLC (gradient: 5–25% B in 20 min): t_R = 13.69 min. ESI-MS: *m/z* =1705.7 $[M + H]^+$, 853.2 $[M + H]^{2+}$, 569.3 $[M + 2H]^{3+}$. HRMS: calcd. for $C_{69}H_{89}N_{39}O_{15}$ $[M + 4H]^{4+}$ 426.94228; found 426.94228.

EXAFS Measurements: An X-ray absorption spectrum at the Cu-*K* edge for oligomer **10** was recorded in fluorescence mode at the EMBL beamline D2 (DESY, Hamburg, Germany) equipped with a Si(111) double crystal monochromator, a focusing mirror and a 13 element Ge solid-state fluorescence detector (Canberra). The Cu-peptide solution was filled into plastic sample holders covered with polyimide windows, frozen in liquid nitrogen, and kept at 30 K during the experiment. Harmonic rejection was achieved by a focusing mirror with a cut-off energy of 21 keV and a monochromator detuning to 70% of peak intensity. A dead-time correction was applied. Saturation was not observed because the dead-time was always below 20%. The energy axis of each scan was calibrated by using the Bragg reflections of a static Si(220) crystal in back reflection geometry.[23] Averaging of 12 scans and data reduction was performed with the EXPROG software package (C. Hermes and H. F. Nolting, EMBL, Hamburg) using $E_{0,Cu}$ = 8979 eV. The EXAFS spectrum was analysed with EXCURV98.[24]

Acknowledgments

Generous support from the Deutsche Forschungsgemeinschaft (SFB 416, project A14) is gratefully acknowledged.

[1] a) K. Tanaka, M. Shionoya, *J. Org. Chem.* **1999**, *64*, 5002–5003; b) K. Tanaka, A. Tengeiji, T. Kato, N. Toyama, M. Shiro, M. Shionoya, *J. Am. Chem. Soc.* **2002**, *124*, 12494–12498; c) K. Tanaka, A. Tengeiji, T. Kato, N. Toyama, M. Shionoya, *Science* **2003**, *299*, 1212–1213.

[2] a) H. Weizman, Y. Tor, *Chem. Commun.* **2001**, 453–454; b) H. Weizman, Y. Tor, *J. Am. Chem. Soc.* **2001**, *123*, 3375–3376.

[3] a) E. Meggers, P. L. Holland, W. B. Tolman, F. E. Romesberg, P. G. Schultz, *J. Am. Chem. Soc.* **2000**, *122*, 10714–10715; b) S. Atwell, E. Meggers, G. Spraggon, P. G. Schultz, *J. Am. Chem. Soc.* **2001**, *123*, 12364–12367; c) N. Zimmermann, E. Meggers, P. G. Schultz, *J. Am. Chem. Soc.* **2002**, *124*, 13684–13685; d) L. Zhang, E. Meggers, *J. Am. Chem. Soc.* **2005**, *127*, 74–75.

[4] a) H.-A. Wagenknecht, *Angew. Chem.* **2003**, *115*, 3322–3324; *Angew. Chem. Int. Ed.* **2003**, *42*, 3204–3206; b) M. Shionoya, K. Tanaka, *Curr. Opin. Chem. Biol.* **2004**, *8*, 592–597.

[5] a) P. E. Nielsen, M. Egholm, O. Buchardt, *Bioconjugate Chem.* **1994**, *5*, 3–7; b) B. Hyrup, P. E. Nielsen, *Bioorg. Med. Chem.* **1996**, *4*, 5–23; c) P. E. Nielsen, M. Egholm, *Curr. Issues Mol. Biol.* **1999**, *1*, 89–104.

[6] P. Bigey, S. H. Sönnichsen, B. Meunier, P. E. Nielsen, *Bioconjugate Chem.* **1997**, *8*, 267–270.

[7] D.-L. Popescu, T. J. Parolin, C. Achim, *J. Am. Chem. Soc.* **2003**, *125*, 6354–6355.

[8] A. Whitney, G. Gavory, S. Balasubramanian, *Chem. Commun.* **2003**, 36–37.

[9] A. Mokhir, R. Stiebing, R. Krämer, *Bioorg. Med. Chem. Lett.* **2003**, *13*, 1399–1401.

[10] a) J. Brunner, A. Mokhir, R. Krämer, *J. Am. Chem. Soc.* **2003**, *125*, 12410–12411; b) F. H. Zelder, J. Brunner, R. Krämer, *Chem. Commun.* **2004**, 902–903.

[11] O. Kornyushyna, A. J. Stemmler, D. M. Graybosch, I. Bergenthal, C. J. Burrows, *Bioconjugate Chem.* **2005**, *16*, 178–183.

[12] a) A. Hess, N. Metzler-Nolte, *Chem. Commun.* **1999**, 885–886; b) R. Hamzavi, T. Happ, K. Weitershaus, N. Metzler-Nolte, *J. Organomet. Chem.* **2004**, *689*, 4745–4750.

[13] a) F. H. Zelder, A. A. Mokhir, R. Krämer, *Inorg. Chem.* **2003**, *42*, 8618–8620; b) A. Mokhir, R. Krämer, H. Wolf, *J. Am. Chem. Soc.* **2004**, *126*, 6208–6209.

[14] K. S. Schmidt, M. Boudvillain, A. Schwartz, G. A. van der Marcel, J. H. van Boom, J. Reedijk, B. Lippert, *Chem. Eur. J.* **2002**, *8*, 5566–5570.

[15] U. Diederichsen, *Angew. Chem.* **1996**, *108*, 458–461; *Angew. Chem. Int. Ed. Engl.* **1996**, *35*, 445–448.

[16] U. Diederichsen, *Angew. Chem.* **1997**, *109*, 1966–1969; *Angew. Chem. Int. Ed. Engl.* **1997**, *36*, 1886–1889.

[17] U. Diederichsen, in *Bioorganic Chemistry − Highlights and New Aspects* (Eds.: U. Diederichsen, T. Lindhorst, L. A. Wessjohann, B. Westermann), Wiley-VCH, Weinheim, **1999**, pp. 255–261.

[18] U. Diederichsen, D. Weicherding, *Synlett* **1999**, *S1*, 917–920.

[19] a) J. Brasuń, P. Ciapetti, H. Kozlowski, S. Oldziej, M. Taddei, D. Valensin, G. Valensin, N. Gaggelli, *J. Chem. Soc., Dalton Trans.* **2000**, 2639–2644; b) J. Brasuń, S. Oldziej, M. Taddei, H. Kozlowski, *J. Inorg. Biochem.* **2001**, *85*, 79–87.

[20] For the preparation of alanyl, homoalanyl and norvalyl nucleo amino acids and their oligomerisation, see: U. Diederichsen, D. Weicherding, N. Diezemann, *Org. Biomol. Chem.* **2005**, *3*, 1058–1066.

[21] J. Peisach, W. E. Blumberg, *Arch. Biochem. Biophys.* **1974**, *165*, 691–708.

[22] The sample solution was prepared from 14.2 μL of 10^{-3} M $Cu(ClO_4)_2$ in H_2O/HEPES and a stoichiometric amount of the investigated oligomer. The low concentrations led to significant problems with regard to the signal-to-noise ratio. In addition, aging of the samples could be observed during repeated measurements as well as a slight temperature dependence of the peak intensities in the range from 8 to 180 K (spectra were recorded using the helium temperature control system ER4112HV; not depicted). The latter finding could be a hint of an increased mobility quenching within the glassy samples at lower temperatures (see also: M. F. Ottaviani, F. Montalti, N. Turro, D. A. Tomalia, *J. Phys. Chem. B* **1997**, *101*, 158–166.). A dependence on the pH values of the actual solution is to be expected but was not tested due to the small amount of sample.

[23] R. F. Pettifer, C. Hermes, *J. Appl. Crystallogr.* **1985**, *18*, 404–412.

[24] N. Binsted, R. W. Strange, *Biochemistry* **1992**, *31*, 12117–12125.

Received: May 22, 2005
Published Online: September 12, 2005

